PASSIVE ISLANDING DETECTON METHOD FOR PHOTOVOLTAIC INVERTER BASED ON WAVELET PACKET TRANSFORM AND SUPPORT VECTOR MACHINE

PHƯƠNG PHÁP PHÁT HIỆN TÁCH ĐẢO BỊ ĐỘNG CỦA BỘ NGHỊCH LƯU QUANG ĐIỆN DỰA TRÊN BIẾN ĐỔI GÓI WAVELET VÀ MÁY VÉC TƠ HỖ TRỢ

Do Thanh Hieu[1,*], Nguyen Viet Ngu[1], Pham Van Cuong[2]

DOI: https://doi.org/10.57001/huih5804.2023.215

ABSTRACT

The disadvantage of the existing passive islanding detection methods is a long detection time and a large non detection zone (NDZ), an islanding detection method based on wavelet packet transform and support vector machine (SVM) was proposed. Firstly, the voltage signal of the point of common coupling is gathered, and then the voltage signal is decomposed into different frequency bands by wavelet packet. Secondly, the normalized logarithmic energy entropy of wavelet packet for each band is calculated, and these features are fed into the SVM model. Finally, the SVM model is used for determining whether there is an island phenomenon. The experimental results verify that the proposed method can detect system islanding operation mode is fast and accurate.

Keywords: *Islanding detection, Wavelet packet transforms, support vector machine.*

TÓM TẮT

Nhược điểm của các phương pháp phát hiện tách đảo thụ động hiện có là thời gian phát hiện dài và vùng không phát hiện (NDZ) lớn, do đó một phương pháp phát hiện sự dựa trên biến đổi gói Wavelet và máy véc tơ hỗ trợ (SVM) được đề xuất. Đầu tiên, tín hiệu điện áp tại điểm ghép nối chung được thu thập, sau đó tín hiệu điện áp này được phân tách thành tín hiệu với các dải tần số khác nhau bằng phép biến đổi gói Wavelet. Thứ hai, entropy năng logarit chuẩn hoá của các gói sóng con cho mỗi dải băng tần được tính toán và các đặc trưng này được đưa tới đầu vào mô hình SVM. Cuối cùng, mô hình SVM được sử dụng để xác định xem có hiện tượng tách đảo xảy ra hay không. Kết quả thực nghiệm cho thấy phương pháp đề xuất có thể phát hiện chế độ tách đảo của hệ thống nhanh và chính xác.

Từ khóa: *Phát hiện tách đảo, biến đổi gói Wavelet, máy véc tơ hỗ trợ.*

[1]Faculty of Electronic and Electrical, Hung Yen University of Technology and Education, Vietnam

[2]Hanoi University of Industry, Vietnam

[*]Email: dothanhhieukt@gmail.com

Received: 25/7/2023

Revised: 25/9/2023

Accepted: 25/11/2023

1. INTRODUCTION

As a component in a photovoltaic (PV) power generation system, a grid - connected PV inverter is used to convert direct current (DC) from solar panels into alternating current (AC) which has the same phase and the same frequency as grid voltage, and to feed the AC to a power grid. Islanding phenomenon of grid-connected photovoltaic (PV) inverters refers to their independent operation when the utility is disconnected. The local section energized by self-activated PV inverters becomes an "island" isolated from the remaining power system. Concern about such phenomenon is raised because it causes danger to uninformed maintenance personnel. Therefore, utility-interactive PV system must be equipped with efficient islanding detection methods (IDMs).

A large number of IDMs have been developed [1-11]. Active methods are based on injection of a small disturbance into the system and analyzing the change in output parameters for islanding detection. The Active Frequency Drift (AFD) [1], Sandia Frequency Shift (SFS) [2], Sliding Mode frequency Shift (SMS) [3], Automatic Phase Shift (APS) [4], impedance measurement [5], and high frequency signal injection [6] are typical examples of the active methods. These methods have a small non detection zone (NDZ) but they may deteriorate power quality during normal power system operation. Whereas, the passive methods discriminate islanding from normal condition based on the measurements of system parameters such as voltage, frequency, etc., at the point common coupling (PCC). The signal parameter measurements or some features are extracted from them are compared to the predetermined threshold. Some passive methods that have been reported consisting of under/over voltage protection and under/over frequency protection (UVP/OVP and UFP/OFP) [7], rate of change of frequency [8], voltage and power factor change [9], etc. Passive methods are easy to

implement, and being grid friendly as no additional signal is injected. However, they fail to detect islanding when the local load consumption closely matches the power output of the DG thus resulting in a large NDZ.

To decrease NDZ of the passive methods modern signal-processing tools such as short-time Fourier transform (STFT), wavelet transform (WT) have been utilized. WT-based techniques discussed in [10, 11] attempt to detecting power islands through the changes that occur in high-frequency components in the measured signals, such as voltages, currents, and frequency. However, the WT only extracts the low frequency sub-band, so it ignores some useful properties of the high frequency band, which has meaning values to reveal islanding condition. Alternatively, wavelet packet transform (WPT) has been applied which has the ability to extract all the low-and high frequency sub-bands of the input signal over all the time-frequency.

In order to further improve the accuracy of islanding detection, this paper proposes an islanding detection method that combines wavelet packet transform and support vector machine. The WPT is used to decompose the components of different frequency bands, and the logarithmic energy entropy of the different frequency band components is used as the input of the support vector machine (SVM) to identify the islanding and non-islanding states of the system. The experimental results verify that the method has the advantages of high islanding detection accuracy, small detection blind area, and fast detection speed.

2. MATERIALS AND METHODS

2.1. Wavelet Packet Transform

The WPT is one type of wavelet-based signal processing that offers a detailed localized time-frequency analysis of discrete-time signals. This analysis is obtained as a result of successive time localization of frequency sub-bands generated by tree of low-pass and high-pass filters. The algorithm is to decompose one node into two nodes step-by-step, i.e., subdividing the whole frequency band of the sampled signal into small segments. Figure 1 shows the wavelet packet decomposition tree with WPT coefficients at each decomposition level j and frequency sub-band n.

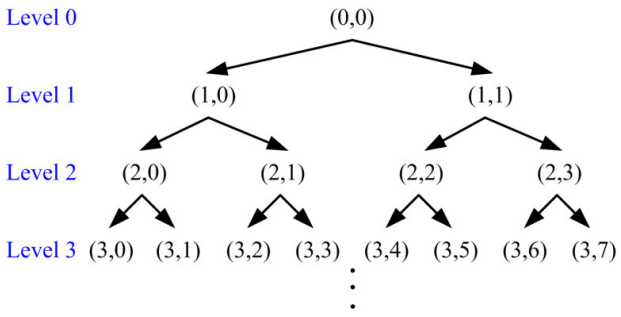

Figure 1. Illustrative diagram of the wavelet packet decomposition

The WPT is a generalization of the WT, and the wavelet packet function is also a time-frequency function, it can be defined as:

$$W_{j,k}^{n}(t) = 2^{\frac{j}{2}} W^{n}\left(2^{j}t - k\right) \quad (1)$$

where the integers j and k are the index scale and translation operations; n is an operation oscillation parameter.

The first two wavelet packet functions expressed as bellow:

$$W_{0,0}^{0}(t) = \phi(t) \quad (2)$$

$$W_{0,0}^{1}(t) = \psi(t) \quad (3)$$

where $\phi(t)$ and $\psi(t)$ are the scaling and mother wavelet functions, respectively.

When n = 2, 3… the function can be defined by the following recursive relationships

$$W_{0,0}^{2n}(t) = \sqrt{2}\sum_{k} h(k) W_{1,k}^{n}(2t-k) \quad (4)$$

$$W_{0,0}^{2n+1}(t) = \sqrt{2}\sum_{k} g(k) W_{1,k}^{n}(2t-k) \quad (5)$$

where $h(k) = 1/\sqrt{2}\left\langle \varphi(t), \varphi(2t-k)\right\rangle$ and $g(k) = 1/\sqrt{2}\left\langle \psi(t), \psi(2t-k)\right\rangle$ are the filter coefficients of low-pass and the high-pass filters respectively, and they are orthogonal with the relationship $g(k) = (-1)^{k} h(1-k)$.

The wavelet packet coefficients (WPCs) $S_{j,k}^{n}$ are obtained by the inner product between the signal x(t) and the wavelet packet functions $W_{j,k}^{n}$ as below:

$$S_{j,k}^{n} = \left\langle x, W_{j,k}^{n}\right\rangle = \int_{-\infty}^{+\infty} x(t) W_{j,k}^{n}(t)\,dt \quad (6)$$

The signal logarithmic energy entropy for each frequency sub-band n and j level is calculated as:

$$E_{j,n} = \sum_{i=1}^{N} \log\left[\left(S_{j,k}^{n}(i)\right)\right]^{2} \quad (7)$$

where N is the number of sampling point, $S_{j,k}^{n}$ is the WPCs at the n^{th} frequency sub-band on the j^{th} level, $n = 2^{j} - 1$.

Also, for better demonstration of the distributed situation of the total signal logarithmic energy entropy in each frequency band, the normalized logarithmic energy entropy (NLEE) value is given by:

$$E_{n} = \frac{E_{j,n}}{\sum_{n=0}^{2^{j}-1} E_{j,n}} \quad (8)$$

2.2. Support Vector Machine Classifier

Support Vector Machine (SVM) is a machine learning algorithm developed on the basis of statistical learning theory based on the principle of structural risk minimization. At present, SVM has been successfully applied in many fields such as power system fault diagnosis and load forecasting [12].

SVM has been developed by Vapnik [13] and is becoming a popular machine learning tool due to great ability to generalize performances. Its principle is based on the

structural risk minimization (SRM) that minimizes an upper bound on the expected risk, opposed to the error on the training data used by neural network (NN). While NN performance is dependent on the size of the training data set and has a number of parameters that should be tuned, SVM may make good prediction using smaller data sets and has fewer parameters to be adjusted.

Given a training set of instances and class label pairs (x_i, y_i), i = 1, 2,..., l, where $x_i \in R^n$ and $y_i \in (1,-1)^l$, the SVM requires the solution of the following optimization problem:

$$\min_{w,b,\xi} \frac{1}{2}\|w\|^2 + C\left(\sum_{i=1}^{l} \xi_i\right) \quad (9)$$

subject to

$$y_i\left[w^T\phi(x_i)+b\right] \geq 1-\xi_i, \quad (\forall i)\ \ \xi_i \geq 0 \quad (10)$$

Here training vectors x_i are mapped into a higher dimensional space by the function ϕ. In the training process the support vectors from the training data will be selected and used to predict unseen data. Parameter C > 0 is the penalty factor of the error term and may be seen as factor that controls the tradeoff between separation margin and training errors, while $\|w\|$ is a norm to the vector perpendicular to the separation hyperline and ξ_i are slack variables which measure degree of misclassification.

Furthermore, $K(x_i,y_i) = \phi(x_i)^T \phi(x_j)$ represents the kernel function. Despite many kernels being proposed by researchers, in this paper radial bias function (RBF).

$$K(x_i,y_i) = e^{-\gamma\|x_i-x_j\|^2}, \quad \gamma > 0 \quad (11)$$

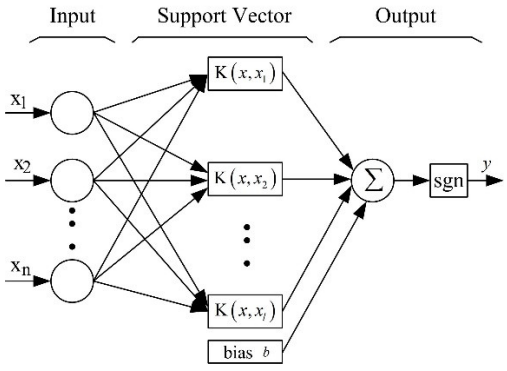

Figure 2. Structure diagram of support vector machine

C and γ can be determined experimentally through a grid search and cross-validation process. To estimate the best values of the C and γ parameters the values of both parameters are varied in increments of the power of 2. For the any parameter combination a k-fold cross-validation is applied. First, the training data set is divided into k subsets of equal size. The SVM classifier is then trained k times and in the lth iteration, l = 1, 2, . . ., k, the classifier is trained using all subsets except the lth subset. The trained classifier is then tested using only the lth subset, and the classification error for this subset is calculated. In such a way, each training subset is tested once, and the cross-validation accuracy is the percentage of the data which are correctly classified.

Finally, the average of these errors is taken as the expected prediction error. This procedure is repeated for the available C and γ parameter values and the best pair that gives the highest estimation accuracy is selected.

Structure diagram of support vector machine is shown in Figure 2.

2.3. Proposed Methodology

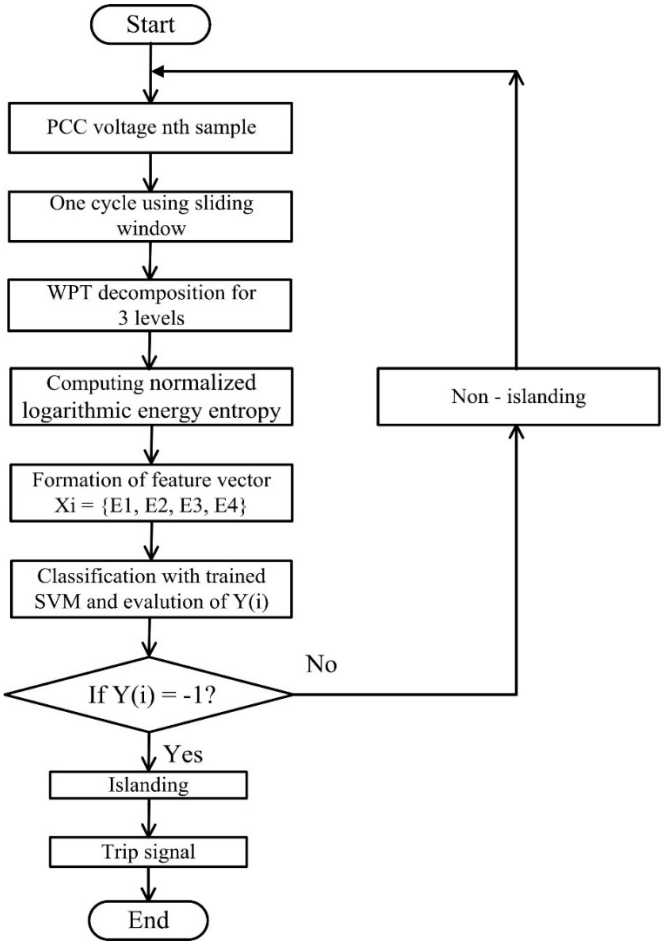

Figure 3. Structure diagram of support vector machine

The purpose of the feature extraction is to identify specific signature of the PCC voltage signal that will help in distinguishing between islanding and non-islanding condition. In this study, the PCC voltage signal is decomposed by WPT which chooses Daubechie's 5 (db5) and the layer of decomposition are 3. The sampling frequency is 10kHz. Therefore, the PCC voltage signal is decomposed into 8 frequency bands. According to the results in [14], the NLEE values of the node (3,1), (3,2), (3,3), and (3,4) are used to feed the SVM for training and testing. The situations that could be present during islanding and non-islanding condition are as follow:

- Trip the utility breaker to island the DG along with active power mismatch from -40% to 40%.

▪ Trip the utility breaker to island the DG along with reactive power mismatch from -40% to 40%.

▪ Trip the utility breaker to island the DG along with active power mismatch from -10% to 10% and reactive power mismatch from -10% to 10%.

▪ Sudden load change at PCC.

▪ Various load quality factors.

▪ Capacitor bank switching.

In order to design and evaluate proposed method, 240 different islanding and non-islanding events are simulated. There are 120 islanding and 120 non-islanding events.

The proposed method can be described in two stages. The first stage involves the training of SVM with different features obtained under several islanding and non-islanding conditions. In the second stage, the trained SVM is applied to detect islanding in real time. The step-by-step procedure of real-time islanding detection is shown in the flowchart presented in Figure 3.

2.4. Hardware Configuration

A 1.2-kW single-phase grid-connected inverter of system shown in Figure 4 was built in the laboratory to verify the performance of the proposed technique. The parameters used in the experiment are provided in Table 1. Figures 4 and 5 show an overall block diagram of hardware and the photograph of the experimental setup for testing the proposed method in the laboratory, respectively. The control system was implemented using a 32-bit digital signal processor (DSP) TMS320F28335 of Texas Instruments, including the inverter controller with the necessary islanding algorithm.

All blocks in the dotted line shown in Figure 1 have been fully carried out by the DSP. In Figure 4, the outputs of the control board consist of signals for the driver board and the trip signal to control a relay RL. The switching off of the utility breaker CB is used to simulate the islanding condition. Furthermore, the dc-link voltage, the PCC voltage and the inverter output current were measured using voltage and current sensors, and fed to the analog-to-digital (A/D) converter ports of the DSP board.

Table 1. System parameters for experiment

No.	Parameter	Value	Unit
1	DC voltage V_{dc}	400	V
2	Rate power of inverter	1200	W
3	Filter inductor Lf	5	mH
4	Filter Capacitor Cf	3	μF
5	Resistance load	40.333	Ω
6	Inductance load	128.4	mH
7	Capacitance load	78.919	μF
8	Quality factor	1	
9	Nominal grid voltage	220	V
10	Grid frequency	50	Hz

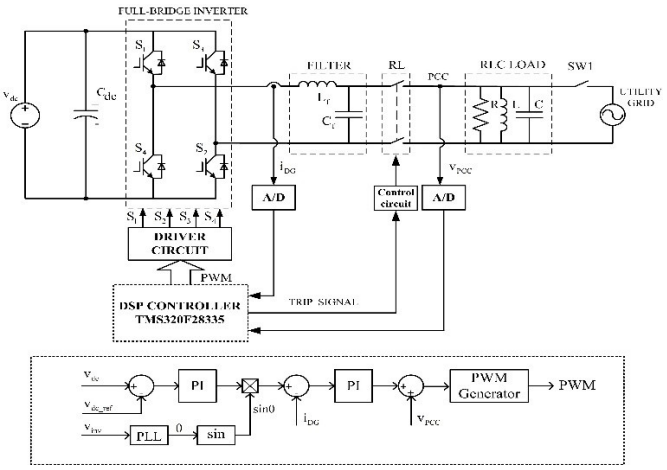

Figure 4. Overall block diagram of the hardware of the experimental setup

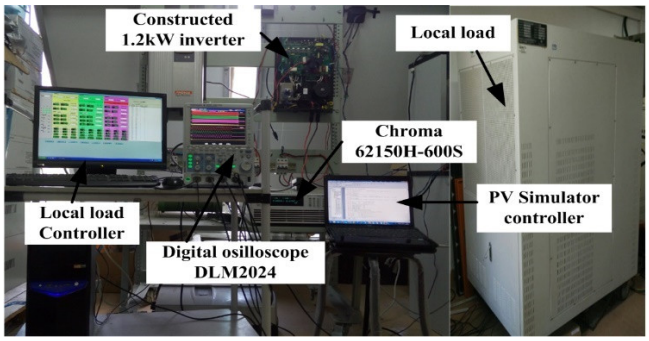

Figure 5. Photograph of the experimental setup in the laboratory

3. RESULTS AND DISCUSSION

When the power of the local load is designed to match the generation power of the PV inverter, the islanding detection is extremely difficult. According to IEC Std. 62116, three typical worst-case studies were considered to prove the effectiveness of the proposed algorithm as follows:

○ Case A: Inverter output power is equal 100%, and ΔP is set to 0%; ΔQ is set to -5% of inverter output power.

○ Case B: Inverter output power is equal 66%, and ΔP is set to 0%; ΔQ is set to +1% of inverter output power.

○ Case C: Inverter output power is equal 33%, and ΔP is set to 0%; ΔQ is set to +1% of inverter output power.

The three cases, in the above-mentioned simulation, were verified by hardware experiment. The obtained experimental results are shown in Figures 6 - 8. Where: Channel CH1 corresponds to the measured voltage waveform at the PCC. Channel CH2 shows the inverter output current waveform. Channel CH3 shows the grid current waveform, and channel CH4 is the trip signal, which simulates the grid disconnection.

Responses of the system for case A, case B, and case C are shown in Figures 6, 7, and 8, respectively. In these cases, the PV inverter is working at 100%, 66%, and 33% of its rated power. From Fig. 6 and 7, when the grid is connected, the grid current is close to zero because in these cases the active consumption power of the local load is designed to match the PV inverter output active power. Whereas, once the islanding occurs, the grid current is immediately equal to

zero. The instant islanding is formed which can be identified at the moment the grid current is dropped to zero.

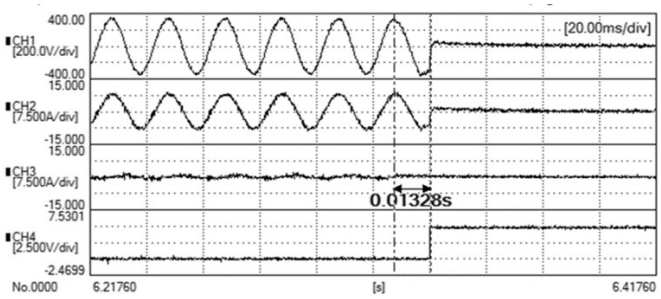

Figure 6. Experimental waveform of islanding detection by the proposed method in condition A

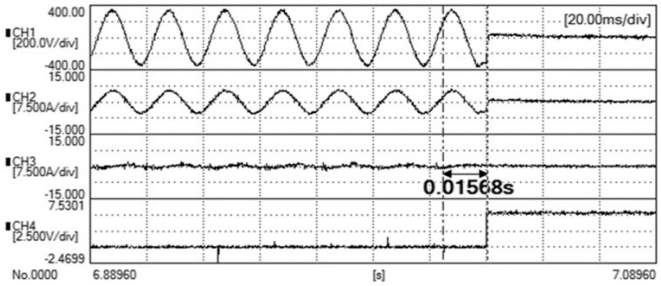

Figure 7. Experimental waveform of islanding detection by the proposed method in condition B

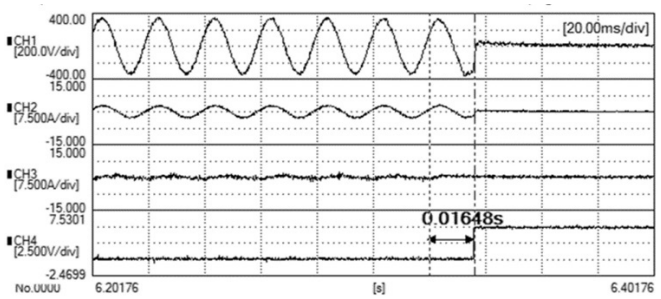

Figure 8. Experimental waveform of islanding detection by the proposed method in condition C

The results indicated that after the islanding is detected, the PV inverter is stopped immediately and the inverter output current and the load current are zero as well. The needed times for the detection of the islanding phenomenon in case A, case B, and case C are 13.28ms, 15.68ms, and 16.48ms, respectively, which are less than 2s in the Std. IEC 62116.

4. CONCLUSION

This paper presents a passive islanding detection method for the grid - connected PV inverter system. The proposed method works based on wavelet packet transform and support vector machine. Experimental results show that this method can quickly and effectively detect islanding under the worst conditions defined in the IEC 62116 standard. In addition, the method has the following characteristics:

1. The proposed method is fast and detection time does not depend on the real/reactive power mismatch.

2. No disturbance is added to the control signal, which will not adversely affect the power quality.

ACKNOWLEDGMENT

This work was supported by the Ministry of Education and Training of Vietnam under Project B2021-SKH-01.

REFERENCES

[1]. Y. Jung, J. Choi, B. Yu, G. Yu, J. So, J. Choi, 2005. *A Novel Active Frequency Drift Method of Islanding Prevention for the grid-connected Photovoltaic Inverter*. Power Electronics Specialists Conference 2005. PESC '05. IEEE 36th, pp. 1915-1921, 16-16.

[2]. M. V. G. Reis, T. A. S. Barros, A. B. Moreira, P. S. Nascimento F., E. Ruppert F., M. G. Villalva, 2015. *Analysis of the Sandia Frequency Shift (SFS) islanding detection method with a single-phase photovoltaic distributed generation system*. 2015 IEEE PES Innovative Smart Grid Technologies Latin America (ISGT LATAM), pp. 125-129.

[3]. B. Singam, L.Y. Hui, 2006. *Assessing SMS and PJD Schemes of Anti-Islanding with Varying Quality Factor*. in Proc. IEEE Int. PECon '06, pp. 196-201.

[4]. Guo-Kiang Hung, Chih-Chang Chang, Chern-Lin Chen, 2003. *Automatic phase-shift method for islanding detection of grid-connected photovoltaic inverters*. in IEEE Transactions on Energy Conversion, vol. 18, no. 1, pp. 169-173.

[5]. D. Zhang, L. Yu, X. Wen, B. Xu, J. Ding, C. Luo, 2019. *Islanding Detection Method for Inverter Cluster Based on Interharmonic Impedance Measurement*. 2019 IEEE 3rd Conference on Energy Internet and Energy System Integration (EI2), pp. 883-888.

[6]. D. Reigosa, F. Briz, C. Blanco, P. García, J. Manuel Guerrero, 2014. *Active Islanding Detection for Multiple Parallel-Connected Inverter-Based Distributed Generators Using High-Frequency Signal Injection.* in IEEE Transactions on Power Electronics, vol. 29, no. 3, pp. 1192-1199.

[7]. H.H. Zeineldin, J.L. Kirtley, 2009. *Performance of the OVP/UVP and OFP/UFP Method with Voltage and Frequency Dependent Loads*. IEEE Trans. Power Del., vol. 24, no.2.

[8]. W. Freitas, X. Wilsun, C.M. Affonso, Huang Zhenyu, 2005. *Comparative analysis between ROCOF and vector surge relays for distributed generation applications*. IEEE Trans. Power Del., vol. 20, no. 2, pp. 1315 – 1324.

[9]. J. Bashir, P. Jena, A. K. Pradhan, 2014. *Islanding detection of a distributed generation system using angle between negative sequence voltage and current*. 2014 Eighteenth National Power Systems Conference (NPSC), pp. 1-5.

[10]. H. Kazemi Karegar, B. Sobhani, 2012. *Wavelet transform method for islanding detection of wind turbines.* Renewable Energy, vol. 38, no. 1, pp. 94-106.

[11]. A. Pigazo, M. Liserre, R. Mastromauro, V. Moreno, A. DellAquila, 2009. *Wavelet-based islanding detection in grid-connected PV systems.* IEEE Trans. Ind. Electron., vol. 56, no. 11, pp. 4445-4455.

[12]. Yufei Wang, Chunguo Wu, Liming Wan, Yanchun Liang, 2010. *A study on SVM with feature selection for fault diagnosis of power systems.* 2010 The 2nd International Conference on Computer and Automation Engineering (ICCAE), pp. 173-176.

[13]. V. Vapnik, 1999. *The Nature of Statistical Learning Theory*. New York, NY, USA: Springer.

[14]. H. T. Do, X. Zhang, N. V. Nguyen, S. S. Li, T. T. Chu, 2016. *Passive-Islanding Detection Method Using the Wavelet Packet Transform in Grid-Connected Photovoltaic Systems.* in IEEE Transactions on Power Electronics, vol. 31, no. 10, pp. 6955-6967.

THÔNG TIN TÁC GIẢ

Đỗ Thành Hiếu[1], Nguyễn Viết Ngư[1], Phạm Văn Cường[2]

[1]Khoa Điện - Điện tử, Trường Đại học Sư phạm Kỹ thuật Hưng Yên

[2]Trường Đại học Công nghiệp Hà Nội